Vol. 656: 19–33, 2020
https://doi.org/10.3354/meps13523

MARINE ECOLOGY PROGRESS SERIES
Mar Ecol Prog Ser

Published December 10

Stoichiometry of Fe, Mn and Co in the marine diazotroph *Crocosphaera subtropica* ATCC51142 in Fe- and P-limited continuous cultures

Alexandra Marki[1], Robert Fischer[2], Thomas J. Browning[1], Evangelia Louropoulou[1], Robert Ptacnik[2], Martha Gledhill[1,*]

[1]GEOMAR Helmholtz Centre for Ocean Research Kiel, Wischhofstr. 1–3, 24148 Kiel, Germany
[2]WasserCluster Lunz-Biologische Station GmbH, Dr. Carl Kupelwieser Promenade 5, 3293 Lunz am See, Austria

ABSTRACT: We investigated trace element stoichiometries of the nitrogen-fixing marine cyanobacterium *Crocosphaera subtropica* ATCC51142 under steady-state growth conditions. We utilized exponentially fed batch cultures and varied iron (Fe) concentrations to establish nutrient limitation in *C. subtropica* growing at a constant growth rate (0.11 d^{-1}). No statistical difference in cell density, chlorophyll *a*, particulate organic carbon (C), nitrogen (N) and phosphorus (P) were observed between consecutive days after Day 14, and cultures were assumed to be at steady state with respect to growth for the remaining 11 d of the experiment. Cultures were limited by P in the highest Fe treatment (41 nmol l^{-1}) and by Fe in the 2 lower-concentration Fe treatments (1 and 5 nmol l^{-1}). Cell size and *in vivo* fluorescence changed throughout the experiment in the 1 nmol l^{-1} Fe treatment, suggesting ongoing acclimation of *C. subtropica* to our lowest Fe supply. Nevertheless, Fe:C ratios were not significantly different between the Fe treatments, and we calculated an average (±SD) Fe:C ratio of 32 ± 14 µmol mol^{-1} for growth at 0.11 d^{-1}. Steady-state P-limited cells had lower P quotas, whilst Fe-limited cells had higher manganese (Mn) and cobalt (Co) quotas. We attribute the increase in Mn and Co quotas at low Fe to a competitive effect resulting from changes in the supply ratio of trace elements. Such an effect has implications for variability in elemental stoichiometry in marine phytoplankton, and potential consequences for trace metal uptake and cycling in marine systems.

KEY WORDS: Nutrient limitation · Cyanobacteria · Trace elements · Elemental stoichiometry · Manganese · Cobalt

1. INTRODUCTION

Nutrient requirements, light and temperature are critical factors determining growth of phytoplankton in the ocean. Quantification of minimum nutrient requirements with regards to the limiting nutrient and growth kinetics under variable nutrient supply are therefore important for accurate parameterisation of phytoplankton elemental stoichiometry in (global) biogeochemical models (Follows & Dutkiewicz 2011, Tagliabue et al. 2016). Steady-state conditions are useful for establishing minimum nutrient requirements in phytoplankton (Bull 2010, Fischer et al. 2014, Henley 2019). Fundamental understanding of nutrient requirements and competition for resources have thus been underpinned by monoculture and competition studies of laboratory phytoplankton cultures that are growing at steady state using continuous culturing approaches (Monod 1950; and see e.g. Droop 1973, Sommer 1986). Continuous cultures may reach steady-state conditions and have the advantage that a response to variations in the abundance of

*Corresponding author: mgledhill@geomar.de

one nutrient substrate can be investigated whilst the abundance of other substrates is kept constant (Bull 2010, Henley 2019). Continuous culturing techniques have thus been applied to the investigation of marine phytoplankton macro-nutrient (nitrogen [N], phosphorus [P] and silica) requirements for more than 70 yr but are nevertheless still less popular than semi-continuous or batch methods, likely because they can be prone to microbial contamination and are more difficult to set up and maintain (Fischer et al. 2014, Henley 2019).

The importance of trace nutrients, such as iron (Fe), cobalt (Co) and manganese (Mn), in determining marine phytoplankton productivity has become increasingly apparent in the last 30 yr (Sunda 1988, Martin et al. 1994, Moore et al. 2013, Tagliabue et al. 2017). Fe is a cofactor in proteins involved in photosynthesis, N fixation and respiration (Geider & La Roche 1994, Moore et al. 2013, Hogle et al. 2014), whilst Co is an essential ion in vitamin B_{12}, and Mn is used to catalyze redox reactions, for example in photosystem II (da Silva & Williams 2001). Phytoplankton in approximately 30% of the surface ocean is directly limited by Fe, and Fe availability also plays a role in controlling community composition and the extent of diazotrophy (Moore et al. 2009, Ward et al. 2013, Hutchins & Boyd 2016). Both Co and Mn have also been suggested as likely or actual limiting nutrients in certain regions of the open ocean (Moore et al. 2013, Browning et al. 2017). These developments have led to a need to incorporate trace nutrient requirements into global biogeochemical models (Ye et al. 2009, Tagliabue et al. 2016, 2018, Weber et al. 2018).

Trace nutrient requirements and extended elemental stoichiometries (i.e. the elemental stoichiometry beyond C:N:P ratios; Twining & Baines 2013) can be highly flexible, and ideally, incorporation of trace nutrients into biogeochemical models would also account for trait-based adjustments in trace nutrient stoichiometries via, for example, optimality based models (Wirtz & Pahlow 2010, Arteaga et al. 2014, Fernández-Castro et al. 2016, Luo et al. 2019). Construction of such models relies on the establishment of robust subsistence nutrient quotas for different metabolic processes (e.g. photosynthesis, N fixation), which are derived from laboratory studies under controlled steady-state conditions (Wirtz & Pahlow 2010). However, investigations of trace nutrient limitation and requirements in marine phytoplankton are typically undertaken using batch or semi-continuous culture methods (e.g. Sunda 2012 and references therein). Although batch culture methods do not approximate steady state as closely as continuous culturing methods, considerable effort has been expended on achieving balanced growth in semi-continuous cultures (Walworth et al. 2016, Boatman et al. 2018, Jiang et al. 2018, Luo et al. 2019), with a focus on keeping biomass low in order to limit changes in nutrient availability during growth (e.g. Boatman et al. 2017). To our knowledge, only a few studies of nutrient limitation by trace elements in marine phytoplankton have employed continuous culturing techniques (Wilhelm & Trick 1995, Pickell et al. 2009, Trick et al. 2010, Spackeen et al. 2018), and steady-state elemental stoichiometry in individual species grown under trace metal limitation in controlled laboratory studies have yet to be reported. Consequently, there is uncertainty as to whether the available data on extended elemental stoichiometries is representative of subsistence quotas under steady-state conditions (e.g. Ward et al. 2013) and with respect to the underlying relationships between elemental stoichiometry, growth rate and environmental conditions (Finkel et al. 2010).

Studies of extended elemental stoichiometries require high sample volume to culture ratios. Furthermore, control of trace element contamination, which is an inherent problem when working with trace nutrient concentrations relevant to the marine environment, is vital (Sunda et al. 2005). The most common continuous culture method is the chemostat, which has the disadvantages that it produces low sample volume to culture ratios and is technically challenging, which leads to chemostats being prone to contamination (Bull 2010).

An alternative to chemostats is the exponentially fed batch (EFB) culture (Fischer et al. 2014). In contrast to chemostats, which rely on a constant addition of fresh media and a constant outflow of biomass plus media, EFB cultures have no outflow. Media are added proportionally to the culture volume, and hence media supply rates increase exponentially over time in order to establish a constant dilution rate. The volume of the media thus increases exponentially until a sample is taken, at which point the culture volume is manually set back. This approach provides a relatively large sample volume to culture volume ratio, which is convenient for determination of analytes present at low concentrations relative to biomass and thus has potential for studying extended elemental stoichiometries under steady-state conditions (Fischer et al. 2014).

Here, we applied trace metal clean conditions to EFB cultures in order to acquire extended elemental ratios for a marine phytoplankton growing under steady-state conditions. We applied the approach to

study the response of the diazotroph *Crocosphaera subtropica* ATCC51142 (synonymous with *Cyanothece* sp. ATCC51142) (Welsh et al. 2008, Mareš et al. 2019) to Fe limitation. *C. subtropica* is a UCYN-C diazotroph closely related to open ocean UCYN-C species (Taniuchi et al. 2012, Mareš et al. 2019). This species is also well characterized (Stöckel et al. 2008, Welsh et al. 2008, Taniuchi et al. 2012), making it a good candidate for establishing new experimental approaches in the laboratory. Nevertheless, fewer studies of Fe limitation in UCYN-C type cyanobacteria have been undertaken (Berman-Frank et al. 2007) in comparison to UCYN-B (Saito et al. 2011, Jacq et al. 2014) or filamentous cyanobacteria (e.g. Kustka et al. 2003, Jiang et al. 2018, Qu et al. 2019). We chose to investigate an N-fixing cyanophyte (diazotroph) because diazotrophs undertake the fixation of large amounts of atmospheric N_2, which is a major input source of new biologically fixed N into the upper water column of the open ocean (Zehr et al. 2001, Moisander et al. 2010, Sohm et al. 2011), and it is thus important to have robust experimental systems for determination of e.g. subsistence nutrient quotas (Landolfi et al. 2015, 2018). The specific aims of our study were thus (1) to examine the suitability of EFB cultures for establishing steady-state Fe limitation, (2) to investigate how steady-state Fe quotas vary with Fe supply at constant growth rate and (3) to investigate the impact of Fe limitation on the elemental stoichiometry of a unicellular marine cyanophyte.

2. MATERIALS AND METHODS

We followed trace metal clean protocols throughout the study (Sunda et al. 2005). All manipulations of culture media and samples were performed under a laminar flow hood equipped with a high-efficiency particulate air filter. All materials were acid washed with 1.2 mol l^{-1} HCl and rinsed with ultrapure water (Milli-Q, MQ) prior to use, with the exception of the sterile culture flasks which were used as supplied by the manufacturer. MQ water (≤18 MΩ cm^{-1}; Millipore) was used to prepare YBCII culture medium (Chen et al. 1996) with a 5 µmol l^{-1} P (as PO_4^{3-}) amendment. The detailed YBCII recipe can be found in Table S1 in the Supplement at www.int-res.com/articles/suppl/m656p019_supp.pdf. Salts were analytical reagent grade and were not purified further, leading to a background Fe concentration of ca. 1 nmol l^{-1}, which was sufficiently low to induce Fe limitation in this diazotroph. The concentration of background Fe was determined in the media prior to the addition of the metal EDTA salts by flow injection analysis according to Obata et al. (1993). We applied 3 treatments: 1 with no Fe addition and 2 where Fe was added as a complex with EDTA at concentrations of 4 and 40 nmol l^{-1} Fe; these Fe treatments are referred to as 1, 5 and 41 nmol l^{-1} treatments, respectively. On preparation, the media were adjusted to pH 8.15–8.24 by addition of 0.01 mol l^{-1} sodium hydroxide (NaOH) and filter sterilised with disposable rapid-flow filter units (PES, 0.1 µm, Nalgene).

Prior to setting up the EFB cultures, the unicellular diazotroph *Crocosphaera subtropica* was maintained in the exponential growth phase in semi-continuous batch cultures (1900 ml, polystyrene, Nunc, Thermo) in triplicate at the relevant Fe concentrations for at least 7 generations. Cells were inoculated into fresh media every 8 d to a cell density of 20 000 cells ml^{-1}. The semi-continuous batch cultures served to determine a common dilution rate for all 3 Fe treatments. *C. subtropica* in the 1 nmol l^{-1} Fe batch cultures showed the lowest maximum growth rates in semi-continuous batch cultures (~0.12 d^{-1}) amongst the 3 Fe treatments and thus determined the common daily dilution rate (D = 0.11 d^{-1}) in the EFB cultures. We also used the cells from semi-continuous cultures to perform a batch culture experiment for comparison with our EFB experiment. Conditions for the batch culture were as close as possible to the EFB conditions. The batch culture experiment was carried out at 25°C in a climate chamber (Sanyo) equipped with cool white fluorescent lights (110–140 µmol photons m^{-2} s^{-1}). For the batch culture, *C. subtropica* was allowed to grow for more than 11 d through to the late exponential phase. The starting volume was 1900 ml, and 300 ml were removed at each sampling time point.

EFB cultures were carried out as described by Fischer et al. (2014). The YBCII culture medium reservoirs consisted of 10 l, high-density polyethylene carboys (Nalgene; n = 3). Fresh YBCII medium was fed through narrow bore polypropylene tubing (inner diameter 0.51 mm, Ismaprene, Pharmed) and a transparent medium injector tube (Tygon LMT 55) into 9 sterile culture flasks (1900 ml, Nunc) using a high-precision 16-channel peristaltic pump (IPC-N, Ismatec). The peristaltic pump was controlled by a programmable microcontroller (Raspberry Pi3), automatically increasing the flow rate (µl min^{-1}) in relation to the current culture volume, in order to ensure a constant common dilution rate. The EFB cultures were carried out in a walk-in environmental chamber at a constant temperature of 25°C. The

ProFiLux Plus II illumination system controlled a light:dark (L:D) cycle of 12:12 h and supplied horizontal light at a light intensity of 140 µmol photons m^{-2} s^{-1}. The panel was equipped with different fluorescent tubes (1 SOLAR ultra NATUR 9000K and 3 SOLAR ultra JBL Tropic 4000K) in order to mimic the spectral quality of natural sunlight. EFB cultures started with an initial volume of 1400 ml and were inoculated with *C. subtropica* to produce an initial cell density of ca. 50 000 cells ml^{-1}. This inoculum resulted in a total particulate Fe carryover of ca. 1 nmol l^{-1}. EFB cultures were gently shaken by hand twice a day and prior to each sampling in order to homogenize the cultures.

The EFB cultures were sampled approximately 2 h after the initiation of the light cycle. This starting volume allowed for sampling approximately 350 ml from each EFB culture every other day. At this point, each EFB culture volume was set back to the initial starting volume of 1400 ml. We subsampled for the determination of cell density, *in vivo* fluorescence, particulate organic C and N (POC and PON), total particulate P (TPP), chlorophyll *a* (chl *a*) and extended elemental stoichiometry (total particulate trace elements).

Cell densities were determined by flow cytometry (Cytoflex, Beckman Coulter). *C. subtropica* was detected using manual gating after visual inspection of the dot plot of red fluorescence (detection: 690 ± 50 nm) versus right angle side scatter. *In vivo* fluorescence and quantum yield (λ = 620 nm) were determined after dark acclimation for at least 30 min using a handheld fluorometer (AquaPen-C; Photon System Instruments). Fluorescence of sterile YBCII media was below detection limits. We used 3 µm calibration beads to estimate cell diameters from forward scatter.

Culture media (50 ml) were filtered for analysis of POC, PON, TPP and chl *a* on precombusted (450°C, 3 h) glass fibre filters (GFF, ∅ 25 mm, 0.7 µm, Whatman) by vacuum filtration (Millipore 1225 Sampling Vacuum Manifold). Filters were stored frozen at –20°C prior to analyses. POC and PON were determined with an elemental analyser (Euro Elemental Analyser), using acetanilide as standard. Filtrates for dissolved inorganic macro-nutrients, total dissolved oxidised inorganic N (nitrate+nitrite) and dissolved inorganic P (DIP) were collected in 15 ml centrifuge tubes and stored at 4°C in the dark prior to analyses using an automated sequential analyser (Quaatro, SEAL Analytic). Chl *a* was determined within 48 h of sampling by fluorescence after extraction into 6 ml 10:90 (volume/volume) H_2O: acetone at –20°C for at least 24 h (Holm-Hansen et al. 1965). Chl *a* extracts were brought to room temperature in the dark prior to determination of chl *a* fluorescence (F7000 Fluorescence Spectrophotometer, INULA Instrumentelle Analytic). Chl *a* from spinach (Sigma Aldrich) was used as a standard. TPP was determined manually after ashing filters at 550°C for 12 h. Phosphate was redissolved at 96°C (1 h) in sulphuric acid (0.09 mol l^{-1}) before dilution (1:10, MQ) and analysis using the spectrophotometric phosphomolybdate assay (Koroleff 1983).

Total particulate concentrations of trace metals were determined after acid digestion by inductively coupled plasma mass spectrometry (Element XR, Thermo). Samples (50 ml) were filtered onto acid cleaned (0.1 mol l^{-1} HCl) polyethylsulphone filters (∅ 25 mm, 0.45 µm, Sterlitech) and frozen prior to digestion and analysis. Prior to use, the 15 ml perfluoroalkoxy digestion vials (PFA, Nalgene) were cleaned 3 times by refluxing overnight in 2 mol l^{-1} HNO_3 at 70°C. Cells were digested following the method described by Honey et al. (2013). After digestion, samples were redissolved in 0.34 mol l^{-1} HNO_3 (double distilled) containing 1 µg l^{-1} indium. Procedural filter blanks (n = 29) were obtained by rinsing acid-washed filters with MQ alongside the collection of samples at each sample time point and were digested and analysed alongside samples. Concentrations of the procedural filter blanks are given in Table S2. Trace metals were measured in medium resolution using indium to correct for instrument drift. Concentrations were calculated using an external calibration curve ranging from 0.01 to 500 µg l^{-1} made from a commercially available mixed standard (71A, Inorganic Ventures). Only concentrations of Fe, Mn and Co are reported here, since only these elements were present at concentrations significantly above blank levels in digested samples.

Statistical analyses were undertaken in the software package R, version 3.6 (R Development Core Team 2016). The non-parametric Friedman test was used to determine the time range over which no significant differences ($p > 0.01$) in measured parameters were observed. This time range was taken to be the time range at which the cultures were at steady state. Significant differences between treatments were then tested with the non-parametric Wilcoxon test.

3. RESULTS AND DISCUSSION

3.1. Growth, nutrient limitation and quantum yield of *Crocosphaera subtropica* in EFB cultures

EFB cultures are conceptually equivalent to chemostats, and thus allow for (1) variation of the specific

growth rate (μ) without changing medium composition, or (2) fixing μ, but varying the concentration of the limiting substrate (Herbert et al. 1956, Bull 2010). In our experiments, we fixed the dilution rate and thus steady-state μ, in order to investigate changes in extended elemental stoichiometry in *C. subtropica* resulting from variations in Fe supply rate. We used the growth rate of Fe-limited *C. subtropica* observed in semi-continuous batch cultures to estimate a dilution rate that was just below the critical dilution rate, thus avoiding wash-out of the cultures (Fig. 1A). Since the dilution rate was close to the observed growth rate for the 1 nmol l^{-1} Fe treatment, we observed only small changes in cell densities and chl *a* in this treatment. In contrast, we observed an exponential increase in cell densities in both the 5 and 41 nmol l^{-1} Fe treatments until nutrient limitation set in (Fig. 1A). A repeated measures Friedman test showed no significant difference ($p > 0.01$) in cell densities in any of the treatments after Day 14, which we thus take here as the onset of steady-state conditions, based on cell densities alone. Our steady-state conditions are thus defined by the time period over which measured growth rates were not significantly different from the dilution rate. Steady-state cell densities were approximately 5 times higher in the 41 nmol l^{-1} treatment than in the 5 nmol l^{-1} treatment, and 14 times higher than the 1 nmol l^{-1} treatment (Table 1). Observation of phosphate concentrations suggested that the 41 nmol l^{-1} treatment was P-, rather than Fe-, limited (Fig. 1B,C). Nitrate+nitrite concentrations were below 0.2 μmol l^{-1} throughout the experiment (Table S3). Quantum yield increased in the 5 nmol l^{-1} treatment until Day 10, before decreasing to similar values as for the 1 nmol l^{-1} treatment (Fig. 1D). Although cell densities reached steady state by Day 14, variability in quantum yield was observed until Day 18 in the 1 and 5 nmol l^{-1} treatments, suggesting that a longer experimental duration may be required to obtain full acclimation of the photosynthetic apparatus to Fe limitation.

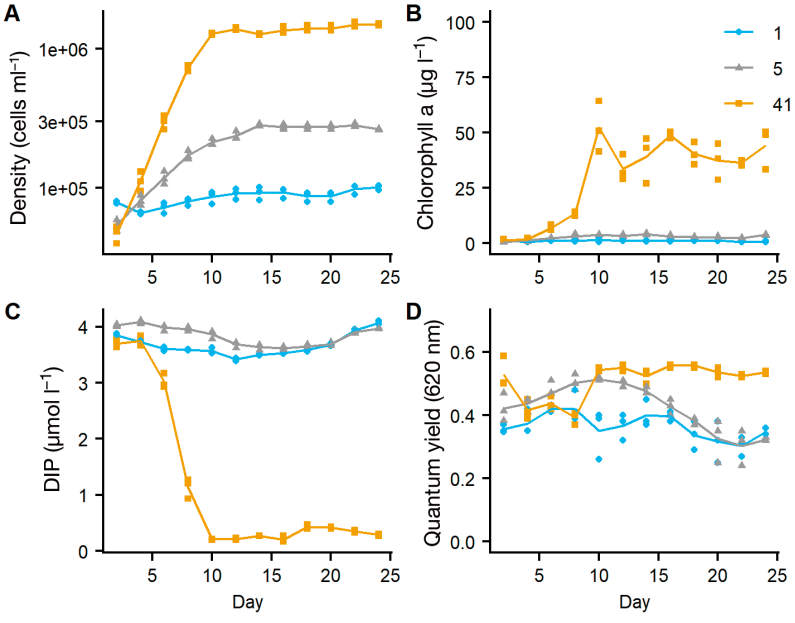

Fig. 1. (A) Cell densities (cells ml^{-1}), (B) chlorophyll *a* concentration (μg l^{-1}), (C) dissolved phosphate (as dissolved inorganic phosphorus, DIP) concentration and (D) quantum yield determined for *Crocosphaera subtropica* in exponentially fed batch cultures growing with a constant dilution rate of 0.11 d^{-1} for 24 d with 3 concentrations of Fe (1, 5 and 41 nmol l^{-1}) in the reservoir media. Points show triplicate measurements every other day, and the line maps the change in the mean value with time. Note log scale in panel A

Table 1. Steady-state (Days 14–24) concentrations of parameters determined for exponentially fed batch cultures of *Crocosphaera subtropica* (n = 18). Values are given as mean ± SD

Parameter	1 nmol l^{-1} Fe treatment	5 nmol l^{-1} Fe treatment	41 nmol l^{-1} Fe treatment
Cells × 10^3 (ml^{-1})	93 ± 8	275 ± 10	1403 ± 91
Chlorophyll *a* (μg l^{-1})	1.1 ± 0.4	3.3 ± 0.7	42.6 ± 7.6
Dissolved inorganic P (μmol l^{-1})	3.72 ± 0.22	3.74 ± 0.14	0.33 ± 0.09
Quantum yield (620 nm)	0.35 ± 0.05	0.37 ± 0.07	0.54 ± 0.02
Particulate organic C (μmol l^{-1})	45 ± 5	114 ± 24	847 ± 85
Particulate organic N (μmol l^{-1})	7.3 ± 1.3	15.9 ± 0.9	76.3 ± 5.4
Total particulate P (μmol l^{-1})	0.7 ± 0.1	1.6 ± 0.1	5.2 ± 0.7
Total particulate Fe (nmol l^{-1})	1.5 ± 0.9	3.5 ± 0.8	23.8 ± 2.6
Total particulate Mn (nmol l^{-1})	2.0 ± 0.4	2.4 ± 0.5	13.8 ± 4.7
Total particulate Co (pmol l^{-1})	20.2 ± 0.3	27.6 ± 0.5	116 ± 30

We also observed a gradual change in cell size over the course of the experiment in all treatments (Fig. S1). Cells in the 41 nmol l^{-1} treatment gradually decreased in size, whilst cell size in 1 and 5 nmol l^{-1} limited treatments increased, so that after Day 16, P-limited *C. subtropica* cells were smaller than Fe-limited cells. Decreased cell size is typically associated with optimization of nutrient uptake, since nutrient diffusion rates are directly linked to cell size (Finkel et al. 2010). For example, a previous study of the N-fixing UCYN-B type cyanobacterium *C. watsonii* observed a 2.2-fold decrease in cell size between cells

grown in 400 nmol l^{-1} Fe and those grown at 3.3 nmol l^{-1} Fe in semi-continuous cultures (Jacq et al. 2014). The decrease in cell size observed by Jacq et al. (2014) largely occurred over the Fe concentration range (43–400 nmol l^{-1} Fe) when growth rates did not change. At lower Fe concentrations, comparable to conditions used in our study, growth rates decreased with decreasing Fe concentration and cell size remained unchanged (Jacq et al. 2014). Our conditions are thus consistent with the range of Fe concentrations over which UCYN-type cyanobacteria can no longer reduce cell size to optimize Fe uptake. The relative increase in cell size in our Fe-limited treatment is nevertheless surprising. Recent investigations of proteome responses to nutrient limitation have shown that a primary response of nutrient limitation is upregulation of membrane transporters and that membrane space can thus become a limiting resource (Held et al. 2020). Our observed changes in cell size could therefore be consistent with this recently proposed mechanism (Held et al. 2020), where Fe acquisition is limited by the number of transporters that can be accommodated by the cell membrane (termed membrane crowding) and the cost of decreasing surface area thus outweighs the benefit of increased surface area:volume ratio. Interestingly, the surface area:volume ratio of *C. subtropica* (Fig. S1) is in the range where membrane crowding is predicted to result in a different cell size response for nutrients limited by membrane crowding versus those limited by diffusion (log[surface area:volume] > 0) (Held et al. 2020).

POC concentrations followed the trend observed for cell densities (Fig. 2A). However, steady-state POC $cell^{-1}$, biovolume-normalized C (C l_{cell}^{-1}) and chl *a*:C ratio varied between treatments, and significantly lower values were observed in the 1 and 5 nmol l^{-1} treatments (mean ± SD: 484 ± 50 and 415 ± 88 fmol C $cell^{-1}$; 45.7 ± 6.2 and 38.7 ± 8.7 mol C l_{cell}^{-1}; 2.1 ± 0.8 and 2.4 ± 0.6 mg chl *a* g^{-1} C respectively; n = 18) compared to the 41 nmol l^{-1} treatment (606 ± 73 fmol C $cell^{-1}$; 70 ± 11 mol C l_{cell}^{-1}; 4.2 ± 0.8 mg chl *a* g^{-1} C). Both C $cell^{-1}$ and chl *a*:C ratios in our 41 nmol l^{-1} treatment were similar to previously reported values of 0.6 ± 0.06 pmol C $cell^{-1}$ and 4.9 ± 1.3 mg g^{-1} chl *a*:C for *Cyanothece* sp. ATCC51142 (synonymous with *Crocosphaera subtropica* ATCC-51142) grown under Fe-replete conditions (Eichner et al. 2014), and the observed decrease in chl *a*:C with reduced Fe supply is consistent with previ-

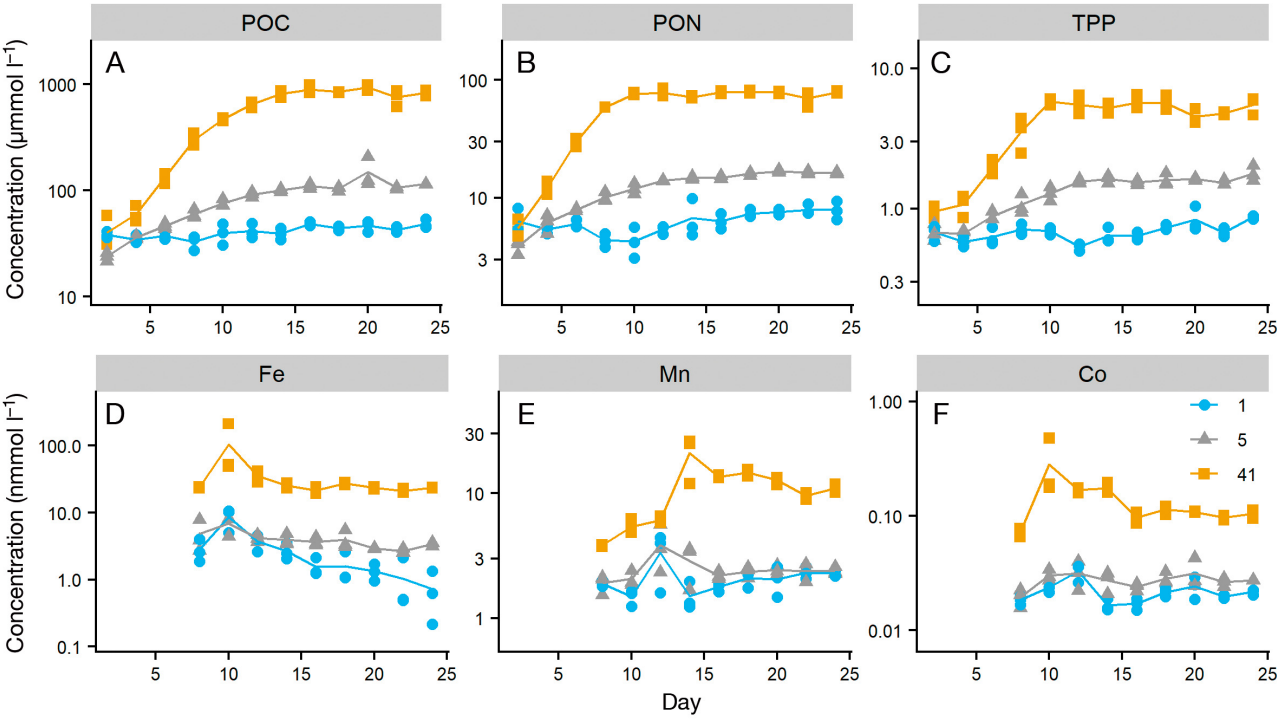

Fig. 2. (A) Particulate organic carbon (POC), (B) particulate organic nitrogen (PON), (C) total particulate phosphorus (TPP), (D) iron, (E) manganese and (F) cobalt concentrations determined for *Crocosphaera subtropica* growing with a constant dilution rate of 0.11 d^{-1} with 3 concentrations of iron (1, 5 and 41 nmol l^{-1}) in the reservoir media. Points show triplicate measurements every other day, and the line maps the change in the mean value with time. Note the log scale for the *y*-axes

ously observed responses to Fe limitation (Sunda & Huntsman 1995). In our experiment, the change in biovolume-normalized C was driven by both changes in POC cell^{-1} and the change in cell volume observed in the different treatments over the course of the experiment. Relationships between cell size, C and chlorophyll content can be influenced by nutrient limitation (Finkel et al. 2010). For example, Sunda & Huntsman (1995) also observed increased cellular C content in Fe-limited eukaryotes with small cell sizes. We cannot fully explain the mechanism behind trends in biomass and cell-normalized nutrient quotas that we observed from our data set, although we note that *C. subtropica* has been shown to produce polyphosphate and carbohydrate granules, which could be expected to impact on both size and cellular C and P content (Schneegurt et al. 1994, Welsh et al. 2008). Further studies investigating the abundance of specific cellular components (e.g. granular bodies, proteins, RNA) are thus required to shed more light on the underlying cause of these changes.

No significant differences in POC, PON and TPP between days were observed after Day 14. In the 41 nmol l^{-1} treatment, the steady-state concentration of TPP was 5.2 ± 0.7 µmol l^{-1} and therefore consistent with complete utilization of the supplied inorganic P (Table 1). We observed some variability in particulate metal concentrations up to Day 14 (Fig. 2). After Day 14, there were no further significant fluctuations in concentrations, although mean particulate Fe concentrations suggested a downward trend may have occurred in the 1 nmol l^{-1} treatment (Fig. 2). Steady-state particulate Fe suggested that a complete drawdown of supplied Fe occurred in the 1 nmol l^{-1} treatment (particulate Fe = 1.5 ± 0.9 nmol l^{-1}) whilst the particulate Fe in the 41 nmol l^{-1} treatment (23.8 ± 2.6 nmol l^{-1}) indicated incomplete Fe drawdown, consistent with P limitation (Table 1).

3.2. Elemental stoichiometry in *C. subtropica*

Elemental ratios varied during non-steady-state growth but did not vary significantly from day to day within treatment post steady state (Fig. 3A–C). C:N ratios varied considerably during non-steady-state growth, potentially as a result of changes in N and C fixation strategies through the growth curve in response to changing Fe and P availability (Schneegurt et al. 1994, Luo et al. 2019). Once steady state was achieved, C:N ratios were higher in the 41 nmol l^{-1} treatment (11.1 ± 0.8 mol mol^{-1}) compared to the 5 and 1 nmol l^{-1} treatments. Comparison with biovolume-normalized cell quotas (Fig. S2) suggests that this change was driven by increased C content in P-limited cells, rather than by changes in N. Ratios of C:P were also higher (164 ± 29 mol mol^{-1}) in the 41 nmol l^{-1} treatment (Fig. 3B), likely driven by both accumulation of C and decreased P in these P-limited cells (Fig. S2). The N:P ratio (14.8 ± 2.1 mol mol^{-1}) was also significantly higher in this treatment compared to the 1 and 5 nmol l^{-1} treatments, consistent with P limitation (e.g. Qu et al. 2019). For the 1 and 5 nmol l^{-1} treatments, we observed similar steady-state C:N:P elemental stoichiometry of 70±15:10±1:1 and 62±9.3:10±2.2:1 respectively, which is also close to that observed previously for *Cyanothece* sp. growing under nutrient-replete conditions in batch culture (Quigg et al. 2011). Our results therefore suggest that P limitation had a stronger influence on C:N:P stoichiometry than Fe limitation at steady state.

Cyanobacteria are able to build up intracellular stores of N, P and/or C, either during diurnal cycles (Schneegurt et al. 1994) or when limited by another nutrient (Kromkamp 1987). The relative changes we observed in our experiments could thus have been influenced by a relative increase in C in P-limited cells linked to an ability to store C under certain conditions, but may also have been influenced by P and N storage under Fe limitation (Kromkamp 1987, Welsh et al. 2008). Our results further suggest that N was not depleted under Fe limitation (Fig. 3), and that N demand was thus met under our low Fe conditions. Here, we note that the overall amount of PON in our 1 nmol l^{-1} treatment did not change over the course of the experiment (Fig. 2; Table S3), and since we did not measure N fixation or ammonium concentrations, we cannot be certain which species of N was utilized to support growth.

In our experiments, *C. subtropica* was able to sustain growth at low total dissolved Fe concentrations (ca. 1 nmol l^{-1}), albeit with relatively low cell densities. C-normalized Fe quotas under steady-state growth were low compared to previous data obtained for *Cyanothece* sp. (Fig. 4; Quigg et al. 2011), but comparable to those obtained for the UCYN-B diazotroph *Crocosphaera watsonii* and the filamentous diazotroph *Trichodesmium* IMS101 when grown at similar Fe concentrations (Kustka et al. 2003, Berman-Frank et al. 2007, Fu et al. 2008), despite the order of magnitude difference in cell volume (5–10 µm^3 for *C. watsonii*, 11 µm^3 for *C. subtropica* and 311 µm^3 for *Trichodesmium*) between the unicellular and filamentous diazotrophs (Berman-Frank et al. 2007, Jacq et al. 2014). Fe:P ratios were also similar to those observed for *Cyanothece* sp. grown at similar Fe con-

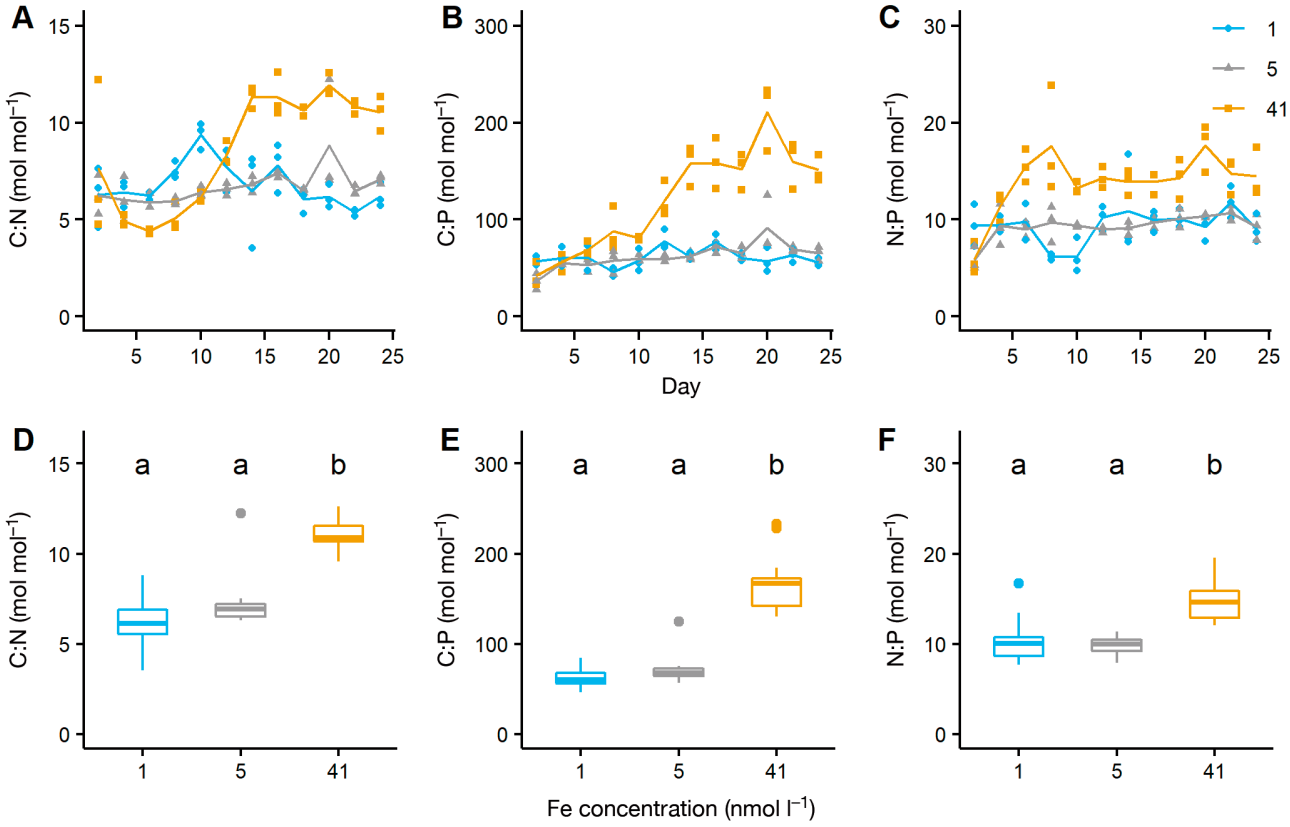

Fig. 3. Elemental ratios determined (A–C) throughout the duration of the exponentially fed batch culture and (D–F) at steady state (after Day 14) for *Crocosphaera subtropica* growing at 0.11 d^{-1} with 3 concentrations of iron (1, 5 and 41 nmol l^{-1}) in the reservoir media. Ratios are carbon:nitrogen (A,D), carbon:phosphorus (B,E) and nitrogen:phosphorus (C,F). Box: 25th–75th percentiles; line inside box: median; whiskers: highest and lowest values, excluding potential outliers (filled dots). Lowercase letters in panels D–F indicate statistically significant differences between treatments ($p < 0.01$, $n = 18$)

centrations (Berman-Frank et al. 2007). We observed elevated concentrations of particulate Fe on Day 10 at the end of the exponential phase (Table S4). We cannot rule out the possibility of contamination of these Day 10 samples during the filtration step; however, since Day 10 was not during the steady-state period, the results obtained on this day are not considered further in our discussion. Typically, Fe:C ratios are observed to decrease as Fe supply decreases (e.g. Sunda & Huntsman 1995, Berman-Frank et al. 2007, Fu et al. 2008). However, previous experiments have employed semi-continuous batch cultures where growth rates and thus Fe demand will also vary in response to changing Fe supply (Raven 1990). In our experiments, growth rate was fixed by the dilution rate, and Fe demand can therefore be expected to be constant in Fe-limited treatments and independent of Fe supply. We thus observed no relationship between Fe supply and C-normalized Fe quota in both Fe-limited treatments (1 and 5 nmol l^{-1}; Fig. 4). Since Fe:C ratios did not increase in the P-limited 41 nmol l^{-1} treatment, our results also suggest that Fe was not stored within the cell under P limitation, a finding consistent with the lack of known Fe storage proteins identified in the *C. subtropica* proteome (Welsh et al. 2008, The UniProt Consortium 2019). This points to fundamental differences in strategy with respect to the response of this organism to macro-nutrient versus Fe limitation that is likely related to its benthic, coastal origin (Reddy et al. 1993).

We furthermore observed constant Fe:C ratios even though cell size and surface area changed across treatments, which can be explained by the fundamental role of Fe in C fixation (Raven 1990). At steady state, C-normalized cell quotas (Q) and net specific rate of C fixation (μ_C) are fundamentally related via the cell C-normalized uptake rate V_M according to the following equation (Sunda 2012)

$$V_M = Q \times \mu_C \quad (1)$$

Application of Eq. (1) to our Fe-limited cultures results in an Fe uptake rate V_M of 4 ± 3 µmol Fe

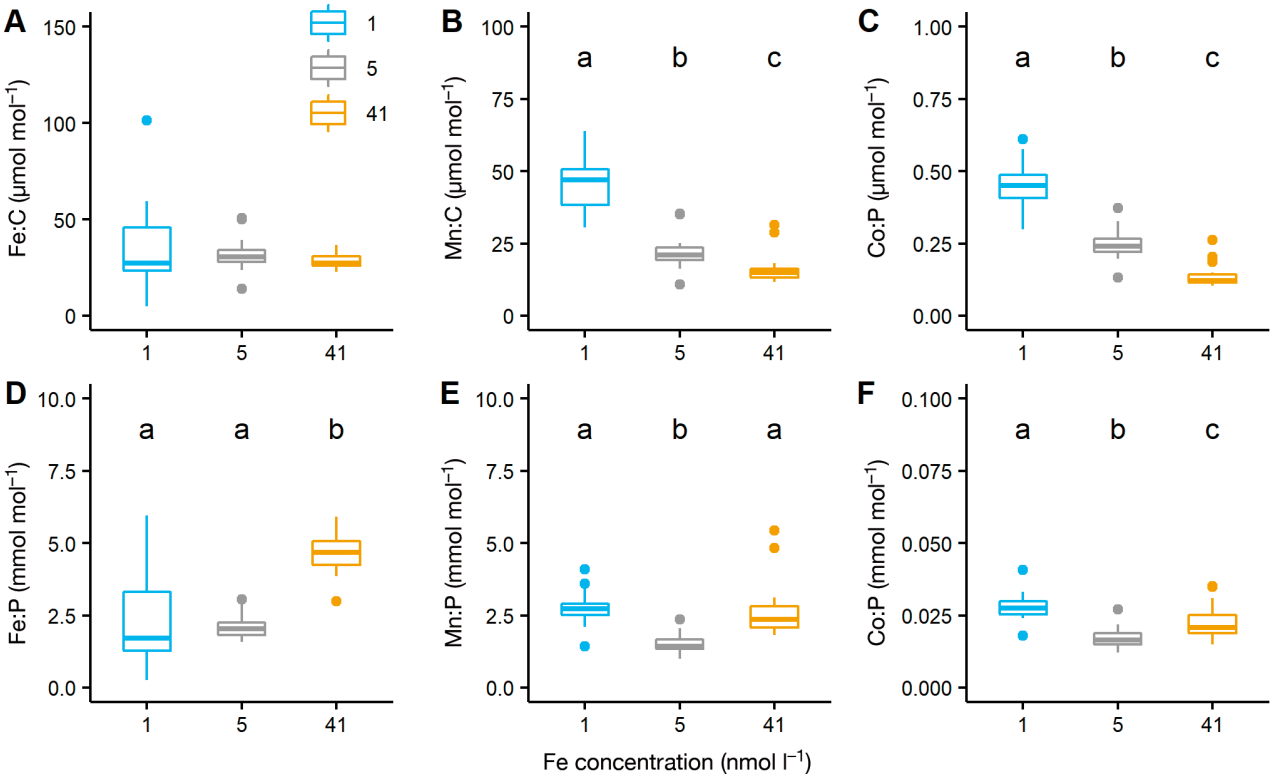

Fig. 4. Elemental ratios determined at steady state (after Day 14) for *Crocosphaera subtropica* growing at 0.11 d^{-1} with 3 concentrations of iron (1, 5 and 41 nmol l^{-1}) in the reservoir media: (A) iron:carbon, (B) manganese:carbon, (C) cobalt:carbon, (D) iron:phosphorus, (E) manganese: phosphorus and (F) cobalt:phosphorus. Boxplot parameters as in Fig. 3. Where shown, lowercase letters indicate statistically significant differences between treatments ($p < 0.01$, $n = 18$)

mol^{-1} C d^{-1} for *C. subtropica*. Thus, we can also conclude that *C. subtropica* did not invoke a high affinity uptake mechanism at low Fe concentrations as has been observed for other species of marine phytoplankton (e.g. Shaked & Lis 2012) and that uptake rates also did not vary with cell size or surface area. Thus, if membrane crowding was behind the increased cell size and surface area in *C. subtropica* in our experiments, it was successful in maintaining Fe homeostasis with respect to C within the cell under our growth conditions, despite the decreased Fe supply. Nevertheless, we note high variability in Fe:C ratios in the 1 nmol l^{-1} treatment (Fig. 4), which likely reflects the increased analytical uncertainty resulting from the low cell densities and thus lower particulate Fe in this treatment and also decreasing trend in particulate Fe that was observed throughout the experiment, despite relatively constant cell densities (Fig. 2). Taken together with the decreasing quantum yield and changes in cell size, this trend could indicate that the phytoplankton were undergoing a longer-term acclimation to the treatment which could ultimately lead to lower C-normalized Fe quotas.

In contrast to Fe, C-normalized Mn and Co quotas significantly increased with decreasing Fe supply (Fig. 4). In the 41 nmol l^{-1} treatment, this trend was likely influenced by the increase in C l_{cell}^{-1} (Fig. S2), but in the 1 nmol l^{-1} Fe treatment, both C and biovolume-normalized cell quotas were higher. *C. subtropica* utilizes an Fe- or Mn-containing superoxide dismutase (The UniProt Consortium 2019), so it is possible that increased Mn could result from metal substitution in this protein, although the relative increase in Mn is greater than the relative decrease in Fe, so the observed increase in Mn cannot be explained by metal substitution alone. Co is not known to substitute for Fe in any proteins, so metal substitution also cannot explain the increase in Co quotas with decreasing Fe concentration in the media. Decreasing trace metal quotas with increasing Fe concentrations have also been attributed to an intracellular dilution effect resulting from combining constant uptake rates with increased growth rates (Sunda 2012). Since steady-state growth rates were constant in our cultures, intracellular dilution of metals resulting from changing growth rates would not explain the observed differences in cellular Mn and

Co quotas observed here, unless there was carry-over from the earlier non-steady-state phase (when growth rates in higher Fe treatments were faster). Therefore, following Eq. (1), we conclude that uptake rates for Mn and Co must have increased in the lowest Fe treatment. Our results could be explained if metal uptake pathways are not completely selective (Sunda & Huntsman 1998, Ma et al. 2009, Hopkinson & Barbeau 2012). In this case, trace metal stoichiometry in the 1 nmol l^{-1} treatment could have influenced cellular stoichiometry via relative increases in the uptake of non-target metals so that their affinities with transporters effectively competed with the transporter's affinity for Fe. This effect could be further enhanced if Fe uptake occurred via a reductive mechanism and transporters were highly upregulated (Hopkinson & Barbeau 2012, Held et al. 2020). Whilst competitive effects between Fe and other metals are considered less likely because of differences in redox state, they have nevertheless been reported for Fe and cadmium (Harrison & Morel 1983), and Fe and copper (Stauber & Florence 1987). To our knowledge, this is the first time such effects have been shown between the trace nutrients Fe, Mn and Co. Nevertheless, such competitive effects have important implications for biogeochemical metal cycling in the ocean (Sunda & Huntsman 1998, Morel et al. 2020), and further work utilizing steady-state conditions in order to disentangle drivers of changing elemental stoichiometries would be useful.

3.3. Comparison with batch cultures

Triplicates of batch cultures were run under similar culture conditions and 3 Fe treatments for 11 d, with 3 sampling points spanning different growth phases (Days 4, 8 and 11), representing the early, mid and late exponential growth phase, respectively. Average growth rate in the batch cultures was determined from cell densities observed over Days 4–8. For EFB cultures, we used cell densities obtained prior to steady-state conditions (Days 4–10) to calculate a non-steady-state growth rate for each treatment after accounting for the dilution rate (Fischer et al. 2014). Results showed that growth rates prior to steady state were similar between culturing methods for each Fe treatment (Table S4), suggesting that overall experimental conditions were consistent in both batch and early-stage EFB cultures. Calculated elemental ratios, however, showed some systematic differences between batch and EFB cultures. Thus, steady-state C:N ratios observed in EFB cultures were not replicated at any one time point in the batch cultures (Fig. 5). Variable C:N ratios were particularly pronounced for batch cultures grown at the lowest Fe concentration. Such transient changes in C:N ratios therefore likely reflect differential optimization of C and N fixation during non-steady-state growth (Schneegurt et al. 1994, Richier et al. 2012, Luo et al. 2019). Steady-state C:P ratios in EFB cultures were similar to those observed in the stationary phase in the batch culture. For the trace nutrients, Fe:C ratios were higher in the 1 nmol l^{-1} treatment in the late exponential phase of the batch cultures. However, we also observed a high variability in Fe:P and Fe:C ratios in our EFB cultures during initial non-steady-state conditions (Tables S3 & S4). This variability in both non-steady-state EFB and in batch cultures likely reflects both changes in micro-nutrient availability and growth strategy as cell densities increase and nutrients are drawn down over the growth curve (Schneegurt et al. 1994, Luo et al. 2019). Increases in Mn:C and Co:C ratios were more pronounced in EFB cultures than in the batch cultures, allowing for increased confidence in the observed relationships (Fig. 4).

3.4. Simulation of EFB cultures

We assessed the consistency of our experimental data against the theoretical behaviour of *C. subtropica* in a steady-state culture by simulating biomass accumulation and changes in P and Fe concentrations over time in our experiment. Using equations describing nutrient dynamics and biomass yield for continuous cultures (e.g. Bull 2010), changes in phytoplankton concentrations (expressed as mol C l^{-1}) in the culture $\frac{dB}{dt}$ were simulated using:

$$\frac{dB}{dt} = \mu_{max} \frac{[N]}{[N]+K_N} B - DB \quad (2)$$

whilst changes in nutrient concentrations $\frac{dN}{dt}$ in the culture were simulated using:

$$\frac{dN}{dt} = -\mu B + D([N_{in}]-[N]) \quad (3)$$

where B is the phytoplankton biomass concentration, $[N]$ is the dissolved nutrient concentration in the culture flask (e.g. Fe or P), $[N_{in}]$ is the dissolved nutrient concentration in the supplied media (i.e. Fe = 5 nmol l^{-1}, P = 5 µmol l^{-1}), D is the dilution rate of nutrients and phytoplankton in the culture flasks by the supplied media (0.11), μ_{max} is the maximum potential phytoplankton growth rate, µ is the

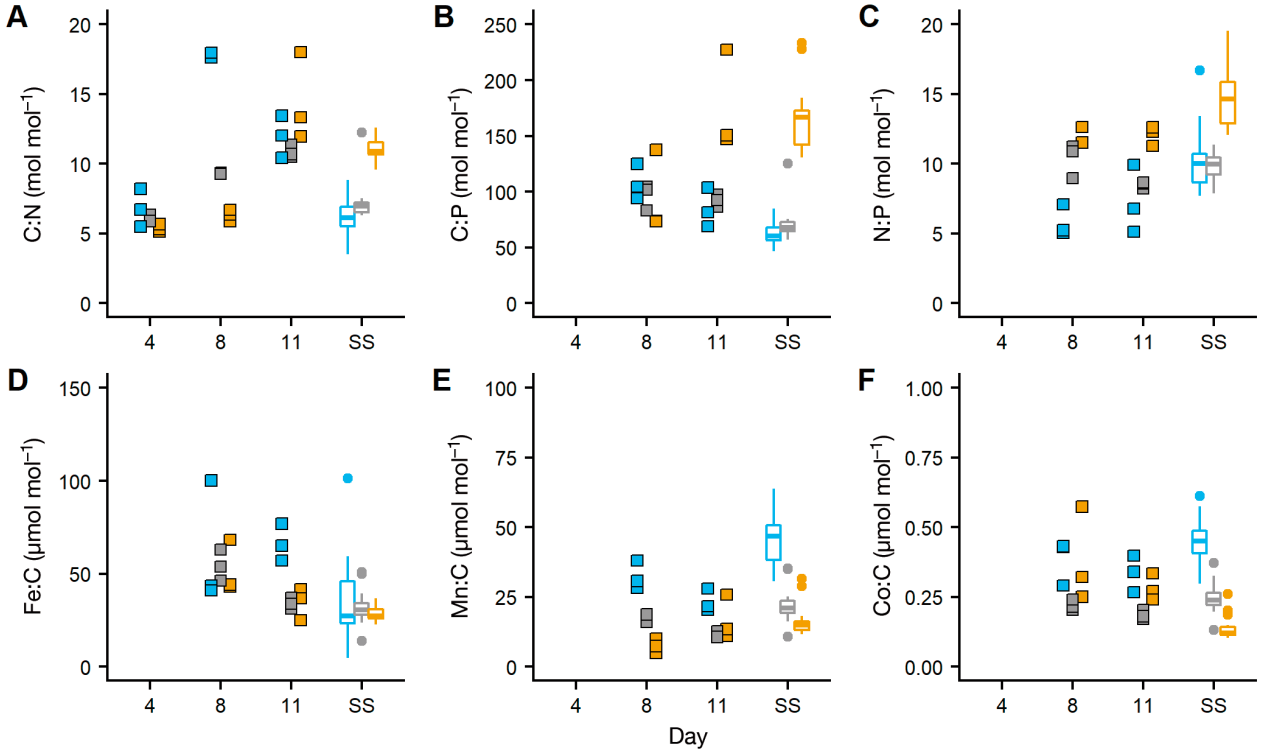

Fig. 5. Elemental stoichiometries observed on Days 4, 8 and 11 in batch cultures and at steady-state (SS) conditions in exponentially fed batch (EFB) cultures of *Crocosphaera subtropica*. Ratios are (A) carbon:nitrogen, (B) carbon:phosphorus, (C) nitrogen:phosphorus, (D) iron:carbon, (E) manganese:carbon and (F) cobalt:carbon. Data for batch cultures are shown as squares, whilst steady state values from EFB cultures are shown as boxes. Boxplot parameters as in Fig. 3. Colours denote the different iron treatments, where blue: 1 nmol l^{-1}, grey: 5 nmol l^{-1} and orange: 41 nmol l^{-1}

achieved phytoplankton growth rate, and K_N is the half-saturation constant for nutrient N. We allowed for growth limitation by either nutrient, with the achieved phytoplankton growth rate calculated using a minimising form of the Michaelis-Menten equation for both nutrients, following Liebig's law of the minimum (e.g. Saito et al. 2008):

$$\mu = min\left(\mu_{max}\frac{[N_1]}{K_{N1}+[N_1]},\ \mu_{max}\frac{[N_2]}{K_{N2}+[N_2]}\right) \quad (4)$$

where $[N_1]$ and $[N_2]$ are the concentrations and K_{N1} and K_{N2} are the half-saturation constants for growth, for nutrients N_1 and N_2, respectively. Assuming the maximum growth rates in our EFB cultures were equal to the growth rate observed in the 41 nmol l^{-1} treatment during non-steady-state exponential growth (0.53 d^{-1}, Day < 10; Table S4), we used the Monod equation (Bull 2010) to obtain a value for K_P = 0.72 µmol l^{-1} and K_{Fe} = 5.2 nmol l^{-1} total dissolved P and Fe, respectively. Although K_N is typically referred to as a constant, it is known to vary considerably with e.g. substrate concentration (Smith et al. 2009) or cell size (Irwin et al. 2006). Nevertheless, the half-saturation constants calculated for P and Fe in our study were within the range of those observed previously for marine diazotrophs (Falcón et al. 2005, Jacq et al. 2014, Lomas et al. 2014).

We then used our calculated K_N and μ_{max} values, measured cellular elemental stoichiometry (176 mol mol^{-1} C:P, 32 µmol mol^{-1} Fe:C) and known nutrient supply rates to simulate *C. subtropica* biomass, growth rates and nutrient substrate concentrations throughout the EFB culture time period (Fig. 6). Simulated biomass corresponded well with observed biomass (Fig. 6A). Simulated growth rates approached the dilution rate in the 5 and 41 nmol l^{-1} treatments (Fig. 6B). The simulation predicted residual Fe (14 nmol l^{-1}; Fig. 6C) and near complete removal of DIP (0.2 µmol l^{-1}) in the 41 nmol l^{-1} treatment, although since we used the P-limited C:P ratio throughout the simulation, DIP depletion was calculated to occur more slowly in the simulation (Fig. 6C). Onset of P limitation in the 41 nmol l^{-1} treatment likely set in at around Day 8–10. According to the simulation, the dissolved Fe:P concentration ratio in the culture media would have increased rapidly at this time (Fig. 6C,D), and it is only after this period that cells could approach steady-state growth in this treatment.

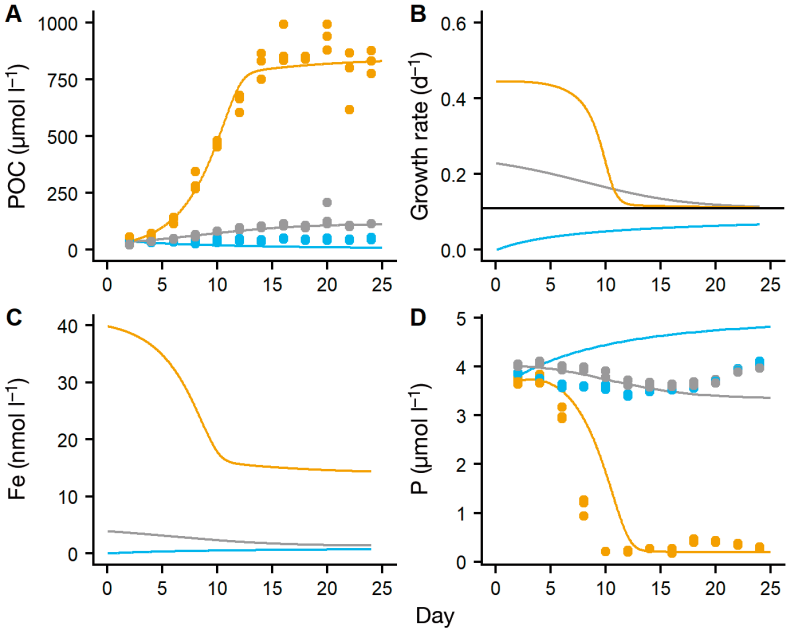

Fig. 6. Simulated response of the exponentially fed batch culture to nutrient availability. (A) Predicted (line) and determined (points) biomass accumulation (expressed as particulate organic carbon, POC). (B) Predicted growth rates with the dilution rate shown by the horizontal black line. (C) Predicted dissolved iron. (D) Predicted (line) and determined (points) dissolved inorganic phosphorus concentrations in the media over the course of the experiment. Colours denote the different iron treatments, where blue: 1 nmol l^{-1}, grey: 5 nmol l^{-1} and orange: 41 nmol l^{-1}

For the 1 nmol l^{-1} treatment, growth rates in our simulation did not reach the dilution rate (Fig. 6B), and the simulation predicted gradually decreasing biomass coupled to gradually increasing Fe and P concentrations, implying wash-out of the culture. However, washout was not supported by our experimental data. Such a discrepancy could have resulted from an underestimate of the Fe concentration supplied in the experiment; our K_{Fe} implies that an Fe supply of 2.5 nmol l^{-1} would be required in order to maintain biomass at the observed level given the average Fe:C ratio. However, both particulate Fe and the quantum yield suggest that *C. subtropica* was undergoing further acclimation to the low Fe treatment that would ultimately lead to lower Fe quotas; for example, our final Fe:C ratio was 15 ± 12 µmol mol^{-1} compared to a ratio of 32 ± 10 µmol mol^{-1} on Day 16. At our dilution rate of 0.1 for 24 d, the duration of our EFB experiment corresponded approximately to 4 generations, which is not considered long enough for full acclimation, which generally takes 6–7 generations or even longer (Boatman et al. 2017, 2018, Qu et al. 2019). We attempted to acclimate our cultures to the Fe treatments via semi-continuous batch cultures for at least 7 generations prior to the start of the EFB cultures. However, batch culture Fe:C ratios did not fall below 25 µmol mol^{-1}, which are still sufficiently high to result in wash-out in the simulation (results not shown). Thus, although cell densities and nutrient inventories suggested that steady-state conditions were established after Day 14, closer examination of elemental stoichiometry, photophysiology and cell size, coupled with simulations of EFB cultures, suggests that a longer experimental period would have been beneficial for assessment of fully acclimated elemental stoichiometry in our lowest Fe treatment.

4. CONCLUSIONS

We applied the EFB culture technique to grow a marine diazotroph under trace metal clean conditions at a constant low growth rate whilst varying Fe supply rate. Steady-state values for biomass (cells ml^{-1} and POC), quantum yield and C:N:P stoichiometry were achieved in 3 different Fe treatments after 14 d. The highest Fe treatment (41 nmol l^{-1}) was P-limited, whilst Fe-limited biomass accumulation was observed in the 2 lower Fe treatments (1 and 5 nmol l^{-1}). Since growth rates were kept constant, steady-state Fe:C ratios were not significantly different between treatments and averaged 32 ± 14 µmol mol^{-1}. We calculated an uptake rate of 4 ± 3 µmol Fe mol^{-1} C d^{-1} and a half-saturation constant of 5.2 nmol l^{-1} total dissolved Fe for *C. subtropica* in our Fe-limited cultures. Elemental stoichiometry was affected by nutrient limitation, with higher C:P and N:P ratios observed in the P-limited treatment and higher Mn:C and Co:C ratios observed in the Fe-limited treatments. Increased Mn:C and Co:C ratios observed at constant growth rates could only be explained by increases in uptake of these trace elements with decreasing Fe supply, which we tentatively attribute to incomplete specificity in uptake mechanisms, combined with upregulation of membrane metal transporters. We noted that a continuing trend of increasing cell size, decreasing quantum yield and decreasing Fe:C ratios in the lowest Fe treatment hinted at possible further acclimation of *C. subtropica* to low Fe availability in these cultures, which may impact on the calculated

half-saturation constant and uptake rate. We observed contrasting responses with respect to cell size, cell quotas and elemental stoichiometries in a comparison of a batch culture with our continuous cultures. These differences also hint at acclimation strategies in this species which were not captured by our semi-continuous batch cultures, possibly because the fluctuations in Fe concentrations that likely occurred in our semi-continuous cultures inhibited longer-term acclimation strategies. The potential for further long-term acclimation of *C. subtropica* in the low Fe treatment was borne out by a simulation of the response of *C. subtropica* to our EFB conditions.

Our study demonstrates the utility of EFB cultures for establishing steady-state responses to Fe limitation and suggests that further application of this method to trace metal limitation studies in marine phytoplankton has the potential to improve knowledge of steady state and subsistence elemental stoichiometries. The high sample volume to culture volume ratio also makes this a suitable method for the investigation of steady-state expression of genes, proteins and metabolites, although the experimental set up requires some specialized equipment. We recommend that sufficient time is allowed for potential acclimation effects to be fully expressed. Overall, we found the EFB approach to be a good alternative to batch cultures for further improving our understanding of trace element controls on ocean productivity.

Acknowledgements. We thank the 2 reviewers for their careful and helpful reviews. This work was funded by the Deutsche Forschungsgemeinschaft as part of Sonderforschungsbereich (SFB) 754: 'Climate-Biogeochemistry Interactions in the Tropical Ocean' and the Integrated Marine Postdoc Network (IMAP, part of the Excellence Cluster 'The Future Ocean'). We thank M. Pahlow for discussions on the manuscript.

LITERATURE CITED

Arteaga L, Pahlow M, Oschlies A (2014) Global patterns of phytoplankton nutrient and light colimitation inferred from an optimality-based model. Global Biogeochem Cycles 28:648–661

Berman-Frank I, Quigg A, Finkel ZV, Irwin AJ, Haramaty L (2007) Nitrogen-fixation strategies and Fe requirements in cyanobacteria. Limnol Oceanogr 52:2260–2269

Boatman TG, Lawson T, Geider RJ (2017) A key marine diazotroph in a changing ocean: the interacting effects of temperature, CO_2 and light on the growth of *Trichodesmium erythraeum* IMS101. PLOS ONE 12: e0168796

Boatman TG, Oxborough K, Gledhill M, Lawson T, Geider RJ (2018) An integrated response of *Trichodesmium erythraeum* IMS101 growth and photo-physiology to iron, CO_2, and light intensity. Front Microbiol 9:624

Browning TJ, Achterberg EP, Rapp I, Engel A, Bertrand EM, Tagliabue A, Moore CM (2017) Nutrient co-limitation at the boundary of an oceanic gyre. Nature 551:242–246

Bull AT (2010) The renaissance of continuous culture in the post-genomics age. J Ind Microbiol Biotechnol 37: 993–1021

Chen YB, Zehr JP, Mellon M (1996) Growth and nitrogen fixation of the diazotrophic filamentous nonheterocystous cyanobacterium *Trichodesmium* sp. IMS 101 in defined media: evidence for a circadian rhythm. J Phycol 32:916–923

da Silva JJRF, Williams RJP (2001) The biological chemistry of the elements: the inorganic chemistry of life, 2nd edn. Oxford University Press, Oxford

Droop MR (1973) Some thoughts on nutrient limitation in algae. J Phycol 9:264–272

Eichner M, Rost B, Kranz SA (2014) Diversity of ocean acidification effects on marine N_2 fixers. J Exp Mar Biol Ecol 457:199–207

Falcón LI, Pluvinage S, Carpenter EJ (2005) Growth kinetics of marine unicellular N_2-fixing cyanobacterial isolates in continuous culture in relation to phosphorus and temperature. Mar Ecol Prog Ser 285:3–9

Fernández-Castro B, Pahlow M, Mouriño-Carballido B, Marañón E, Oschlies A (2016) Optimality-based *Trichodesmium* diazotrophy in the North Atlantic subtropical gyre. J Plankton Res 38:946–963

Finkel ZV, Beardall J, Flynn KJ, Quigg A, Rees TAV, Raven JA (2010) Phytoplankton in a changing world: cell size and elemental stoichiometry. J Plankton Res 32:119–137

Fischer R, Andersen T, Hillebrand H, Ptacnik R (2014) The exponentially fed batch culture as a reliable alternative to conventional chemostats. Limnol Oceanogr Methods 12:432–440

Follows MJ, Dutkiewicz S (2011) Modeling diverse communities of marine microbes. Annu Rev Mar Sci 3:427–451

Fu FX, Mulholland MR, Garcia NS, Beck A and others (2008) Interactions between changing pCO_2, N_2 fixation, and Fe limitation in the marine unicellular cyanobacterium *Crocosphaera*. Limnol Oceanogr 53:2472–2484

Geider RJ, La Roche J (1994) The role of iron in phytoplankton photosynthesis, and the potential for iron limitation of primary productivity in the sea. Photosynth Res 39: 275–301

Harrison GI, Morel FMM (1983) Antagonism between cadmium and iron in the marine diatom *Thalassiosira weissflogii*. J Phycol 19:495–507

Held NA, Webb EA, McIlvin MM, Hutchins DA and others (2020) Co-occurrence of Fe and P stress in natural populations of the marine diazotroph *Trichodesmium*. Biogeosciences 17:2537–2551

Henley WJ (2019) The past, present and future of algal continuous cultures in basic research and commercial applications. Algal Res 43:101636

Herbert D, Elsworth R, Telling RC (1956) The continuous culture of bacteria; a theoretical and experimental study. J Gen Microbiol 14:601–622

Hogle SL, Barbeau KA, Gledhill M (2014) Heme in the marine environment: from cells to the iron cycle. Metallomics 6:1107–1120

Holm-Hansen O, Lorenzen CJ, Holmes RW, Strickland JDH (1965) Fluorometric determination of chlorophyll. ICES J Mar Sci 30:3–15

Honey DJ, Gledhill M, Bibby TS, Legiret FE and others (2013) Heme *b* in marine phytoplankton and particulate

material from the North Atlantic Ocean. Mar Ecol Prog Ser 483:1–17
Hopkinson BM, Barbeau KA (2012) Iron transporters in marine prokaryotic genomes and metagenomes. Environ Microbiol 14:114–128
Hutchins DA, Boyd PW (2016) Marine phytoplankton and the changing ocean iron cycle. Nat Clim Change 6: 1072–1079
Irwin AJ, Finkel ZV, Schofield OME, Falkowski PG (2006) Scaling-up from nutrient physiology to the size-structure of phytoplankton communities. J Plankton Res 28: 459–471
Jacq V, Ridame C, L'Helguen S, Kaczmar F, Saliot A (2014) Response of the unicellular diazotrophic cyanobacterium *Crocosphaera watsonii* to iron limitation. PLOS ONE 9: e86749
Jiang HB, Fu FX, Rivero-Calle S, Levine NM and others (2018) Ocean warming alleviates iron limitation of marine nitrogen fixation. Nat Clim Change 8:709–712
Koroleff F (1983) Determination of total nitrogen and phosphorus. In: Grasshoff K, Erhardt M, Kremling K (eds) Methods for seawater analysis, 2nd edn. Verlag Chemie, Weinheim, p 162–173
Kromkamp J (1987) Formation and functional significance of storage products in cyanobacteria. N Z J Mar Freshw Res 21:457–465
Kustka A, Sañudo-Wilhelmy S, Carpenter EJ, Capone DG, Raven JA (2003) A revised estimate of the iron use efficiency of nitrogen fixation, with special reference to the marine cyanobacterium *Trichodesmium* spp. (Cyanophyta). J Phycol 39:12–25
Landolfi A, Koeve W, Dietze H, Kähler P, Oschlies A (2015) A new perspective on environmental controls of marine nitrogen fixation. Geophys Res Lett 42:4482–4489
Landolfi A, Kähler P, Koeve W, Oschlies A (2018) Global marine N_2 fixation estimates: from observations to models. Front Microbiol 9:2112
Lomas MW, Bonachela JA, Levin SA, Martiny AC (2014) Impact of ocean phytoplankton diversity on phosphate uptake. Proc Natl Acad Sci USA 111:17540–17545
Luo YW, Shi D, Kranz SA, Hopkinson BM, Hong H, Shen R, Zhang F (2019) Reduced nitrogenase efficiency dominates response of the globally important nitrogen fixer *Trichodesmium* to ocean acidification. Nat Commun 10: 1521
Ma Z, Jacobsen FE, Giedroc DP (2009) Coordination chemistry of bacterial metal transport and sensing. Chem Rev 109:4644–4681
Mareš J, Johansen JR, Hauer T, Zima J Jr and others (2019) Taxonomic resolution of the genus *Cyanothece* (Chroococcales, Cyanobacteria), with a treatment on *Gloeothece* and three new genera, *Crocosphaera, Rippkaea*, and *Zehria.* J Phycol 55:578–610
Martin JH, Coale KH, Johnson KS, Fitzwater SE and others (1994) Testing the iron hypothesis in the ecosystems of the equatorial Pacific Ocean. Nature 371:123–129
Moisander PH, Beinart RA, Hewson I, White AE and others (2010) Unicellular cyanobacterial distributions broaden the oceanic N_2 fixation domain. Science 327:1512–1514
Monod J (1950) La technique de culture continue: théorie et applications. Ann Inst Pasteur (Paris) 79:390–410
Moore CM, Mills MM, Achterberg EP, Geider RJ and others (2009) Large-scale distribution of Atlantic nitrogen fixation controlled by iron availability. Nat Geosci 2:867–871
Moore CM, Mills MM, Arrigo KR, Berman-Frank I and others (2013) Processes and patterns of oceanic nutrient limitation. Nat Geosci 6:701–710
Morel FMM, Lam PJ, Saito MA (2020) Trace metal substitution in marine phytoplankton. Annu Rev Earth Planet Sci 48:491–517
Obata H, Karatani H, Nakayama E (1993) Automated-determination of iron in seawater by chelating resin concentration and chemiluminescence detection. Anal Chem 65:1524–1528
Pickell LD, Wells ML, Trick CG, Cochlan WP (2009) A seagoing continuous culture system for investigating phytoplankton community response to macro- and micronutrient manipulations. Limnol Oceanogr Methods 7: 21–32
Qu P, Fu FX, Kling JD, Huh M, Wang X, Hutchins DA (2019) Distinct responses of the nitrogen-fixing marine cyanobacterium *Trichodesmium* to a thermally variable environment as a function of phosphorus availability. Front Microbiol 10:1282
Quigg A, Irwin AJ, Finkel ZV (2011) Evolutionary inheritance of elemental stoichiometry in phytoplankton. Proc R Soc B 278:526–534
R Development Core Team (2016) R: a language and environment for statistical computing. R Foundation for Statistical Computing, Vienna. www.r-project.org
Raven JA (1990) Predictions of Mn and Fe use efficiencies of phototrophic growth as a function of light availability for growth and of C assimilation pathway. New Phytol 116: 1–18
Reddy KJ, Haskell JB, Sherman DM, Sherman LA (1993) Unicellular, aerobic nitrogen-fixing cyanobacteria of the genus *Cyanothece.* J Bacteriol 175:1284–1292
Richier S, Macey AI, Pratt NJ, Honey DJ, Moore CM, Bibby TS (2012) Abundances of iron-binding photosynthetic and nitrogen-fixing proteins of *Trichodesmium* both in culture and *in situ* from the north Atlantic. PLOS ONE 7: e35571
Saito MA, Goepfert TJ, Ritt JT (2008) Some thoughts on the concept of colimitation: three definitions and the importance of bioavailability. Limnol Oceanogr 53:276–290
Saito MA, Bertrand EM, Dutkiewicz S, Bulygin VV and others (2011) Iron conservation by reduction of metalloenzyme inventories in the marine diazotroph *Crocosphaera watsonii.* Proc Natl Acad Sci USA 108:2184–2189
Schneegurt MA, Sherman DM, Nayar S, Sherman LA (1994) Oscillating behavior of carbohydrate granule formation and dinitrogen fixation in the cyanobacterium *Cyanothece* sp. strain ATCC 51142. J Bacteriol 176:1586–1597
Shaked Y, Lis H (2012) Disassembling iron availability to phytoplankton. Front Microbiol 3:123
Smith SL, Yamanaka Y, Pahlow M, Oschlies A (2009) Optimal uptake kinetics: physiological acclimation explains the pattern of nitrate uptake by phytoplankton in the ocean. Mar Ecol Prog Ser 384:1–12
Sohm JA, Webb EA, Capone DG (2011) Emerging patterns of marine nitrogen fixation. Nat Rev Microbiol 9:499–508
Sommer U (1986) Nitrate- and silicate-competition among antarctic phytoplankton. Mar Biol 91:345–351
Spackeen JL, Sipler RE, Bertrand EM, Xu K and others (2018) Impact of temperature, CO_2, and iron on nutrient uptake by a late-season microbial community from the Ross Sea, Antarctica. Aquat Microb Ecol 82:145–159
Stauber JL, Florence TM (1987) Mechanism of toxicity of ionic copper and copper complexes to algae. Mar Biol 94: 511–519

Stöckel J, Welsh EA, Liberton M, Kunnvakkam R, Aurora R, Pakrasi HB (2008) Global transcriptomic analysis of *Cyanothece* 51142 reveals robust diurnal oscillation of central metabolic processes. Proc Natl Acad Sci USA 105:6156–6161

Sunda WG (1988) Trace metal interactions with marine phytoplankton. Biol Oceanogr 6:411–442

Sunda WG (2012) Feedback interactions between trace metal nutrients and phytoplankton in the ocean. Front Microbiol 3:204

Sunda WG, Huntsman SA (1995) Iron uptake and growth limitation in oceanic and coastal phytoplankton. Mar Chem 50:189–206

Sunda WG, Huntsman SA (1998) Processes regulating cellular metal accumulation and physiological effects: phytoplankton as model systems. Sci Total Environ 219:165–181

Sunda WG, Price NM, Morel FMM (2005) Trace metal ion buffers and their use in culture studies. In: Anderson RA (ed) Algal culturing techniques. Elsevier, Burlington, MA, p 35–65

Tagliabue A, Aumont O, DeAth R, Dunne JP and others (2016) How well do global ocean biogeochemistry models simulate dissolved iron distributions? Global Biogeochem Cycles 30:149–174

Tagliabue A, Bowie AR, Boyd PW, Buck KN, Johnson KS, Saito MA (2017) The integral role of iron in ocean biogeochemistry. Nature 543:51–59

Tagliabue A, Hawco NJ, Bundy RM, Landing WM, Milne A, Morton PL, Saito MA (2018) The role of external inputs and internal cycling in shaping the global ocean cobalt distribution: insights from the first cobalt biogeochemical model. Global Biogeochem Cycles 32:594–616

Taniuchi Y, Chen YLL, Chen HY, Tsai ML, Ohki K (2012) Isolation and characterization of the unicellular diazotrophic cyanobacterium Group C TW3 from the tropical western Pacific Ocean. Environ Microbiol 14:641–654

The UniProt Consortium (2019) UniProt: a worldwide hub of protein knowledge. Nucleic Acids Res 47:D506–D515

Trick CG, Bill BD, Cochlan WP, Wells ML, Trainer VL, Pickell LD (2010) Iron enrichment stimulates toxic diatom production in high-nitrate, low-chlorophyll areas. Proc Natl Acad Sci USA 107:5887–5892

Twining BS, Baines SB (2013) The trace metal composition of marine phytoplankton. Annu Rev Mar Sci 5:191–215

Walworth NG, Fu FX, Webb EA, Saito MA and others (2016) Mechanisms of increased *Trichodesmium* fitness under iron and phosphorus co-limitation in the present and future ocean. Nat Commun 7:12081

Ward BA, Dutkiewicz S, Moore CM, Follows MJ (2013) Iron, phosphorus, and nitrogen supply ratios define the biogeography of nitrogen fixation. Limnol Oceanogr 58: 2059–2075

Weber T, John S, Tagliabue A, DeVries T (2018) Biological uptake and reversible scavenging of zinc in the global ocean. Science 361:72–76

Welsh EA, Liberton M, Stöckel J, Loh T and others (2008) The genome of *Cyanothece* 51142, a unicellular diazotrophic cyanobacterium important in the marine nitrogen cycle. Proc Natl Acad Sci USA 105:15094–15099

Wilhelm SW, Trick CG (1995) Physiological profiles of *Synechococcus* (Cyanophyceae) in iron-limiting continuous cultures. J Phycol 31:79–85

Wirtz KW, Pahlow M (2010) Dynamic chlorophyll and nitrogen:carbon regulation in algae optimizes instantaneous growth rate. Mar Ecol Prog Ser 402:81–96

Ye Y, Voelker C, Wolf-Gladrow DA (2009) A model of Fe speciation and biogeochemistry at the Tropical Eastern North Atlantic Time-Series Observatory site. Biogeosciences 6:2041–2061

Zehr JP, Waterbury JB, Turner PJ, Montoya JP and others (2001) Unicellular cyanobacteria fix N_2 in the subtropical north Pacific Ocean. Nature 412:635–638

Editorial responsibility: Toshi Nagata, Kashiwanoha, Japan
Reviewed by: T. Masuda and 1 anonymous referee

Submitted: December 19, 2019
Accepted: October 2, 2020
Proofs received from author(s): November 23, 2020